Validation of MISR Aerosol Optical Thickness Measurements Using AERONET Observations over the Contiguous United States

Yang Liu[1], Jeremy A. Sarnat[2], Brent A. Coull[3], Petros Koutrakis[2] and Daniel J. Jacob[1,4]

[1]Division of Engineering and Applied Sciences, Harvard University, Cambridge, MA 02138

[2]Department of Environmental Health, Harvard School of Public Health, Boston, MA 02215

[3]Department of Biostatistics, Harvard School of Public Health, Boston, MA 02215

[4]Depart of Earth and Planetary Sciences, Harvard University, Cambridge, MA 02138

Abstract. Aerosol optical thickness (AOT) data derived by the Multi-angle Imaging SpectroRadiometer (MISR) from Jan 2001 to Feb 2002 were compared with AOT measurements from 16 Aerosol Robotic Network (AERONET) sites over the contiguous United States. Overall, MISR and AERONET AOTs were strongly correlated (correlation coefficient = 0.81). Regression analysis showed that MISR AOT retrievals had a positive error of approximately 0.10 with no systematic bias across the data range. Importantly, our findings showed that the positive errors in MISR AOT were greater during the spring and summer. Additionally, the presence of coarse particles in the aerosol led to increased errors which weakened the association between MISR and AERONET. Finally, it is unlikely that the current results will vary when using alternative MISR AOT parameters since our analysis also showed the MISR AOT parameters (best fit, regional mean, and weighted regional mean AOTs) to be interchangeable. Together these results suggest that MISR AOT measurements may be suitable for quantitative analysis of aerosol abundance.

1. Introduction

NASA's Earth Observing System (EOS) Terra satellite [*Kaufman et al.*, 1998] was launched into Earth orbit in December 1999 with the mission of comprehensively measuring the Earth's climate system. Operating in a sun-synchronous orbit, Terra crosses the equator from north to south at approximately 10:45 a.m. local time with an orbital period of 99 minutes and repeats its ground track every 16 days. Among the five instruments aboard Terra, MISR [*Diner et al.*, 1989; *Diner et al.*, 1998] was designed mainly for tropospheric aerosol measurements with repeat coverage over a specific scene between two and nine days depend on the latitude of the scene. MISR employs nine cameras pointed at fixed angles to observe reflected sunlight in four wavelength bands. This unique design enables it to retrieve tropospheric AOT, defined as the integral of aerosol extinction coefficients from surface to tropopause, and aerosol size distribution over both land and ocean at a resolution of 17.6 km [*Diner et al.*, 1998]. Unlike other aerosol remote sensing instruments, MISR performs aerosol retrieval over land utilizing the presence of spatial contrasts within the 17.6 × 17.6 km region to separate surface-leaving and atmospheric path radiances. The surface-leaving radiation field is then used to determine the best-fitting aerosol compositional models and associated AOTs by comparing the results with synthesized values which are calculated assuming various aerosol compositional models, each consisting of a mixture of prescribed particles. Valid aerosol models and associated AOTs are identified when the residuals between observed and synthesized radiation fields are below the thresholds specified by a set of chi-squared statistics [*Martonchik et al.*, 1998].

Since MISR is still in its early stage of operation, most existing MISR related publications focus on instrument operations, radiometric and geometric calibrations as well as studies of land surface and cloud properties [*Bruegge et al.*, 2002; *Chrien et al.*, 2002; *Jovanovic et al.*, 2002]. To date, MISR aerosol measurements have been undergoing extensive validation with few published results. *Diner et al.* [2001] compared a small sample of the regional mean aerosol optical depth, computed from early MISR measurements with AOT observations from the Aerosol Robotic Network (AERONET) in southern Africa. Their results showed that MISR had a small positive error (0.02) across the range of the data and overestimated AERONET AOT measurements by 10%.

AERONET is a global measurement network of ground-based sun photometers (CIMEL Electronique, France) supported by NASA's EOS and other international institutions [*Holben et al.*, 1998]. Starting operation in 1993, AERONET has expanded worldwide to over 340 sites by 2002. The AERONET system provides columnar aerosol optical properties at up to eight wavelengths ranging from 340 nm to 1020 nm. Extensive research showed that AERONET data have relatively high accuracy (typically the total uncertainty in AOT under cloud-free conditions is $< \pm 0.01$ for $\lambda > 440$ nm and $< \pm 0.02$ for shorter wavelengths) and precision (less than 1%) [*Eck et al.*, 1999; *Holben et al.*, 1998; *Smirnov*, 2000]. Because of its long operating history, global coverage and high data quality, AERONET data have been used in various satellite and model validation studies as the reference standard for measuring AOT [*Chu et al.*, 2002; *Torres et al.*, 2002a; *Torres et al.*, 2002b; *Zhao et al.*, 2002].

Because of their relatively high resolution and wide coverage over land, the latest generation of spaceborne aerosol sensors such as MISR and Moderate Resolution Imaging Spectroradiometer (MODIS) are promising data sources for regional scale studies on fine particle pollution characterization and related public health issues. A case study in Texas has shown that MODIS, in conjunction with ground-based observations, can create a cost-effective and accurate pollution monitoring system [*Hutchison*, 2003]. MISR or MODIS data may be especially beneficial in developing countries with limited ground monitoring network and financial resources. To date, no study has specifically focused on evaluating MISR data over relatively populated and polluted areas for long sampling durations. The main objectives of this study, therefore, are to validate MISR AOT data over the contiguous United States using information from the AERONET network. More specifically, our analysis will focus on:

- The relationships among different AOT variables provided by the MISR data product;
- The association between AOT measured at 10 - 11a.m. local time and daylight average AOT;
- The overall accuracy of MISR aerosol measurements over continental U.S.; and
- The association between MISR and AERONET AOTs obtained under various geographical and climatic conditions.

2. Methods

2.1 Measurements of AOT

2.1.1 MISR Level 2 Aerosol Data Product

A total of 14 months (Jan 2001 – Feb 2002) of MISR Level-2 aerosol data [*Bothwell et al.*, 2002] were used in this study. Study dates were extended to include January and February 2002 since many MISR orbits from January to February 2001 were not available during data collection. The Terra spacecraft repeats its global coverage cycle every 16 days using the Landsat Worldwide Reference System-2 (WRS-2) numbering system to identify its 233 orbit "paths" during each repeat cycle. In order to cover the entire contiguous U.S., all MISR data during the study period from paths 10 to 46 were downloaded from Atmospheric Sciences Data Center at NASA Langley Research Center. (http://edg.larc.nasa.gov/~imswww/imswelcome/index.html). It should be noted that the MISR aerosol retrieval algorithm as well as the product maturity level have been constantly evolving. In the current analysis, the 2001 data are versions 3 to 6 except March and July (version 9) and the data for January and February of 2002 are versions 10 or 11. The MISR AOT parameters [*JPL*, 2002] of interest include:

- Best-fit AOT indicating the columnar aerosol optical depth with smallest chi-square fitting parameter from all aerosol mixtures [*Martonchik et al.*, 1998]. Denoted as $MISR_{bestfit}$ in this analysis;
- Regional Mean AOT indicating the columnar aerosol optical depth computed as the average optical depths of all valid ("successful") aerosol mixtures. Denoted as $MISR_{regmean}$;

- Weighted Regional Mean AOT indicating the columnar aerosol optical depth computed as the average optical depths for all aerosol mixtures weighted by the inverse of the chi-square statistics. Denoted as $MISR_{wgtdmean}$;
- MISR Retrieval Success Flag reflecting the degree of success in retrieved MISR AOT, where flag = 7 indicates successful retrievals, flag = 8 indicates that there is no successful retrieval and the average from surrounding 8 pixels is given instead. Denoted as $Flag_{MISR}$.

All AOT parameters were reported for the green band (center wavelength 558 nm). In order to spatially match MISR pixels with AERONET sites, the center coordinates of MISR pixels were extracted from MISR Ancillary Geographic Product (AGP).

2.1.2 AERONET Level 2 Data Product

Level-2 (validated) AOT data from January 2001 to February of 2002 from 16 AERONET sites over contiguous United States (Figure 1) were downloaded from the AERONET data archive (http://aeronet.gsfc.nasa.gov). All data were pre- and post- field calibrated and manually inspected. Cloud screening was conducted automatically using threshold criteria related to both short time period (1 minute) as well as hourly and diurnal variation of AOTs [*Smirnov*, 2000]. Each site was assigned a unique ID with the geographical information (i.e., latitude, longitude, elevation, location and land use type) about these sites listed in Table 1. Parameters provided by this AERONET data product include AOTs at different wavelengths, relative errors of AOTs, Angstrom exponents (α) among different bands as well as sampling dates and time.

2.2 Data Analysis

Due to AOT's strong wavelength dependence, the comparison between MISR and AERONET was conducted at the same wavelength to allow for straightforward interpretation of the results. The spectral dependence of AOT was parameterized through the Angstrom exponent (α) defined as:

$$\alpha_{\lambda 1-\lambda 2} = -\frac{d \ln \tau_\lambda}{d \ln \lambda} = -\frac{\ln(\frac{\tau_{\lambda 1}}{\tau_{\lambda 2}})}{\ln(\frac{\lambda 1}{\lambda 2})} \qquad (1)$$

where $\tau_{\lambda 1}$ and $\tau_{\lambda 2}$ were AOTs at wavelengths λ_1 and λ_2 respectively. In this analysis, AERONET AOT at 440 nm and 675 nm were interpolated to 558 nm using the Angstrom exponents ($\alpha_{440-675\ nm}$) provided in the datasets. Given that Terra passes over the U.S. at approximately 10:30 a.m. local time, 10 - 11 a.m. local time was used as MISR measurement time window. Averages of AERONET AOTs measured in this window (denoted as $AERONET_{10am}$ in this analysis) as well as daily means (denoted as $AERONET_{daily}$) were calculated.

The values of $\alpha_{440\text{-}675\ nm}$[1] was also used as a categorical indicator of aerosol size distribution [*Eck et al.*, 1999; *Kaufman et al.*, 2000; *Thulasiraman et al.*, 2002]. For $\alpha_{440\text{-}675\ nm}$ values less than 0.75, desert dust or maritime particles (in super-micron radius range, referred to as coarse particles in this analysis) were dominant. For $\alpha_{440\text{-}675\ nm}$ values greater than 1.7, fresh biomass burning smoke and urban/industrial aerosol (in

---

[1] Because $\alpha_{440\text{-}675\ nm}$ information was not available at Sioux Falls, $\alpha_{440\text{-}870\ nm}$ was used instead.

sub-micron radius range, referred to as fine particles) were dominant. For $\alpha_{440\text{-}675\ nm}$ values between 0.75 and 1.70, a mixture of coarse and fine particles are present. This criterion was used to classify different aerosol size distributions in the analysis.

The coordinates of the AERONET sites were matched with the center coordinates of the corresponding MISR pixels using ArcGIS (ESRI Inc.; Redlands, CA) using Albers Equal Area Conic projection, which preserves distance well at the middle latitudes. For the purpose of this analysis, only records that contained all three valid MISR AOT parameters were included for clear interpretation of the results. Data were characterized using descriptive statistics, graphical displays, goodness-of-fit tests (Kolmogorov-Smirnov test, Cramer-von Mises test and Anderson-Darling test), Spearman's correlation coefficients (to account for the lognormality of the data shown later in the analysis), and simple and general linear regression models. Correlation and regression analyses were conducted using the SAS system (SAS Institute Inc.; Cary, NC) under different climatic and geographical conditions. Statistical significance was reported at 0.05 level.

Results from mixed model regression analysis showed that the association between $MISR_{bestfit}$ and $AERONET_{10am}$ did not differ by site ($p = 0.43$). The data also did not exhibit significant autocorrelation. For the current analysis, the average temporal spacing between two consecutive MISR-AERONET observations for a given site was 20 days, much longer than MISR's global coverage time of 2 - 9 days. This large temporal spacing observed in this dataset is likely because MISR cannot retrieve aerosol properties when either a scene is covered by clouds, the surface is too bright or the terrain lacks spatial contrast. In addition, many of the AERONET sites did not operate during the

entire 14-month sampling period. Based on the above findings, all the data points were considered independent.

2.3 Data Cleaning

Because the accuracy and precision of AERONET data are well documented, most of the data cleaning was conducted for the MISR data. Firstly, since the detection limit (LOD) of the MISR AOT is currently estimated to be 0.025 (David Diner, personal communication), three data points with MISR AOT values below 0.025 were excluded from this analysis. Secondly, as recommended by the MISR science team (David Diner, personal communication), MISR AOTs greater than 1.50 (N = 3) were likely blunders caused by inadequate cloud screening. Therefore, they were removed to reduce possible data contamination. This threshold was justified by the observation that only four out of a total of 81,500 AOT measurements collected at the 16 AERONET sites in 2001 exceeded 1.5 (interpolated to 558 nm). In addition, these four extreme AOTs were all observed on June 29, 2001 at Cove, VA during a strong but short pollution episode dominated by coarse mode particles.

Finally, histograms of MISR data (Figure 2) show that the three AOT parameters exhibited similar mono-modal distributions except for a few points in the right tail of the distribution (all from Walker Branch site, $MISR_{bestfit}$ = 1.30 on March 16, 2001, 1.30 on June 11, 2001 and 1.44 on June 20, 2001). This was highlighted in Figure 3 showing these three data points apparently deviated from the general trend of the entire dataset. As shown in Figure 4, the total precipitable water (TPW) profiles followed closely the variation of AOT during these three periods with elevated water vapor level during the

pollution episodes. Since TPW is a rough indicator of cloud cover, it is likely that either these three records were contaminated by clouds due to inadequate cloud screening before aerosol retrieval or that the MISR retrieval algorithm did not adopt to the rapid change of water vapor effectively. Further analysis was beyond the scope of this paper. After these three records were excluded from the analysis, goodness-of-fit tests indicated that all three parameters followed lognormal distributions which agree with results from a multi-year, multi-station study of AERONET data [*O'Neill et al.*, 2000]. The final dataset was composed of 204 records. Statistical tests were conducted using both log transformed and untransformed AOT parameters yielding very similar results and interpretations. Therefore, only test results on log transformed parameters were reported. Untransformed parameters were selected for the regression analysis to provide clearer interpretation of parameter estimates.

3. Results and Discussion

3.1 Summary Statistics

Summary statistics for the MISR and AERONET AOT values for the entire dataset as well as stratified by season, aerosol size distribution, and by site are presented in Tables 2, 3 and 4 and Figure 5. It clear that the three MISR AOT parameters were highly comparable and so was the two AERONET AOT parameters. MISR AOT values ranged from 0.025 to over 1.0. Paired t-tests on showed that $MISR_{bestfit}$ was significantly greater than $AERONET_{10am}$ ($p < 0.0001$) with a mean difference (± standard deviation) of 0.09 (± 0.01). AOT varied greatly by season and geographic location. The mean values for both MISR and AERONET AOTs were highest during the summer (June through August) and

lowest during the winter (December through February). $MISR_{bestfit}$ was approximately 40% greater than $AERONET_{10am}$ during the spring and summer with a mean AOT difference of 0.12, and 60% greater in fall and winter with a mean AOT difference of 0.05.

The mean MISR and AERONET AOT values were the lowest and least variable under coarse particle dominant conditions. Western sites had lower and less variable AOT values than midwestern and eastern sites due to the lower particle level (Figure 5). The greatest annual mean $MISR_{bestfit}$ value was observed at SERC, MD (0.39 ± 0.31) and so was the greatest annual mean $AERONET_{10am}$ (0.31 ± 0.28). The lowest annual mean $MISR_{bestfit}$ was observed at Rogers Dry Lake, CA (0.13 ± 0.09) while the lowest annual mean $AERONET_{10am}$ was observed at Sevilleta, NM (0.06 ± 0.03). Finally, the mean MISR AOTs of the four urban sites (La Jolla, GSFC, MD Science Center and Philadelphia) were not significantly different from the 12 non-urban sites (t-tests, $p > 0.10$ for all three parameters). However, AERONET AOT values were found to be significantly higher at urban sites than non-urban sites (t-tests, $p < 0.0001$ for both parameters).

3.2 Relationships among MISR AOT Parameters

The relationships among $MISR_{bestfit}$, $MISR_{regmean}$ and $MISR_{wgtdmean}$ were examined using paired t-tests and linear regression analyses. Differences between the paired means for log transformed MISR parameters were significant for $MISR_{bestfit}$ vs. $MISR_{regmean}$ ($p = 0.02$); marginally significant for $MISR_{bestfit}$ vs. $MISR_{wgtdmean}$ ($p = 0.051$); and insignificant for $MISR_{regmean}$ vs. $MISR_{wgtdmean}$ ($p = 0.67$). Differences between the means were less

than 0.01 in both cases. $MISR_{bestfit}$, $MISR_{regmean}$ as well as $MISR_{wgtdmean}$ had excellent 1:1 relationships with small and insignificant or marginally significant intercepts (Figure 6). Given that the LOD of MISR is 0.025, the differences among MISR AOT parameters are practically negligible. When assessed together, the above results show that all three MISR AOT variables are highly comparable and may be used interchangeably.

Since only data points with the three valid MISR parameters were included in the dataset, $MISR_{bestfit}$ for a given data point must be associated to one of the valid aerosol compositional model according to the definitions of these three parameters. Since, on average, there were less than five successful mixtures for each MISR pixel, the excellent agreement between $MISR_{bestfit}$ and $MISR_{regmean}$ seems to indicate that the valid aerosol models for a specific pixel exhibit similar optical properties. The agreement between $MISR_{regmean}$ and $MISR_{wgtdmean}$ is less straightforward with one possible explanation being that aerosol model selection criteria in MISR retrieval algorithm was very sensitive. As a result, the impact of invalid aerosol models accounted in $MISR_{wgtdmean}$ was greatly reduced due to the weighting scheme. For the following analyses, $MISR_{bestfit}$ was chosen as the representative MISR AOT parameter and only its relationship with AERONET AOT variables were assessed.

3.3 Relationship between AERONET AOT Variables

The relationships between $AERONET_{10am}$ and $AERONET_{daily}$ were examined using paired t-tests and simple linear regressions. Since AERONET only operates during daytime (usually 8 – 12 hours depending on location and season), it is impossible to quantify how much MISR AOT will vary from an actual 24-hour average. The difference between the

paired means for log transformed AERONET parameters was insignificant (t-test, p = 0.68). The overall ratio of $AERONET_{10am}$ to $AERONET_{daily}$ had a mean of 1.02 ± 0.02 with a standard deviation of 0.23. This result is consistent with the observations from Kaufman et al. [2000] using multiple years of global AERONET data. Result from simple linear regression analysis between the two AERONET parameters was shown in Figure 7. The slope of 1.08 (± 0.02) indicates that on average $AERONET_{10am}$ systematically overestimates $AERONET_{daily}$ by 6-10% across the range of observed values, which corresponds to a difference of less than 0.01. Given that this difference is comparable to the uncertainty level of AERONET AOT measurements, the two AERONET parameters may be considered interchangeable. To evaluate the quality of MISR AOT, $AERONET_{10am}$ was used study the associations between MISR and AERONET since this parameter more closely corresponds to the time of day when MISR conducts its measurements.

3.4 Association between MISR and AERONET

3.4.1 Correlation Coefficients and Simple Linear Regression Analysis

Overall, there was a strong correlation between $MISR_{bestfit}$ and $AERONET_{10am}$ (r = 0.81, p < 0.0001). All sites with more than nine observations showed significant correlations ranging from 0.51 to 0.94 with the exception of Rogers Dry Lake, CA (p = 0.06). In addition, the correlation at La Jolla, CA was only marginally significant (p = 0.04) (Table 5). The seasonal variation of the correlation at each site was not analyzed due to limited sample size. Since the eastern U.S. generally has higher levels of $PM_{2.5}$ than the midwest and western U.S. [*EPA*, 2001], the influence of measurement errors in

AOT values would influence the correlation between $MISR_{bestfit}$ and $AERONET_{10am}$ more substantially at western U.S. sites than at eastern U.S. sites. As a result, east coast sites had a stronger overall correlation (r = 0.89) as compared to mid west (r = 0.73) and west coast sites (r = 0.54) (Table 6). This may also explain the insignificant correlation at Rogers Dry Lake which has the lowest mean $MISR_{bestfit}$ (0.13 ± 0.09) as well as the weaker and less significant at coastal site La Jolla, CA (N = 9, r = 0.70, p = 0.04) as compared to another coastal site Cove, VA (N = 9, r = 0.74, p = 0.002).

Table 6 showed the differences in the strength of the association between the two AOT measurements by other potential factors. The correlations were stronger during the summer (r = 0.79) as compared to during the spring (r = 0.54) and the fall (r = 0.59), and it was not significant during the winter (r = 0.22, p = 0.21). The insignificant correlation in the winter was shown to be associated with the positive bias in MISR data, which will be discussed in next section.

Although successful MISR aerosol retrievals assume simple and flat terrain, the correlation was stronger at low altitude sites (r = 0.90) than high altitude sites (r = 0.69). This was also illustrated by the higher R^2 values in the simple linear regression of $MISR_{bestfit}$ on $AERONET_{10am}$ when using data from low altitude sites (N = 151, R^2 = 0.66, intercept = 0.10 ± 0.02, slope = 0.94 ± 0.06) as compared to using data from high altitude sites (N = 53, R^2 = 0.28, intercept = 0.09 ± 0.02, slope = 1.10 ± 0.25). Both the intercepts and the slopes in the two cases, however, were not significantly different from each other. Therefore, although MISR data were noisier in higher altitude locations, it was not systematically different from data in lower altitude locations.

Correlation between MISR and AERONET was found to be stronger in the case of $Flag_{MISR} = 8$ (r = 0.83) than $Flag_{MISR} = 7$ (r = 0.58). However, linear regressions yielded similar slopes (0.90 ± 0.08, 0.93 ± 0.07 for $Flag_{MISR} = 8$ and $Flag_{MISR} = 7$ respectively) and intercepts (0.12 ± 0.03, 0.09 ± 0.01 for $Flag_{MISR} = 8$ and $Flag_{MISR} = 7$ respectively). Since MISR is most sensitive to particles between 0.05 and 2 μm [*Kahn et al.*, 1998], the particles it observes are likely to be spatially homogeneous at a scale of larger than 3 × 3 = 9 pixels except for locations with strong local emission sources. The above results suggest that MISR data quality flag does not influence the association between MISR and AERONET and the lower correlation when $Flag_{MISR} = 7$ was likely due to higher noise level in this portion of MISR data.

Stronger correlation was observed at urban sites as a group (r = 0.90) than suburban and rural sites as the other group (r = 0.69). Since the mean $MISR_{bestfit}$ values were comparable in both cases (0.29 ± 0.23 for urban sites, 0.24 ± 0.21 for suburban and rural sites), the difference between the correlation coefficients was not likely the result of different noise levels. It was further examined using general linear regression analysis. The correlation between MISR and AERONET was insignificant in the coarse particle dominant scenario (r = 0.39, p = 0.10) while the correlation coefficients were comparable for the mixed particles scenario (r = 0.75) and the fine particle dominant scenario (r = 0.78). This seems to suggest that the presence of coarse particles might increase the uncertainty in $MISR_{bestfit}$. This observation was further examined using general linear models (GLM).

3.4.2 General Linear Regression Analysis

As shown in the previous section, $Flag_{MISR}$ and *altitude* did not have significant impact on the regression of $MISR_{bestfit}$ against $AERONET_{10am}$. Therefore, these factors were not addressed further in this section. GLMs were used to examine the association between $MISR_{bestfit}$ from $AERONET_{10am}$ and other categorical variables such as season, land use, and aerosol size distribution as well as their interactions with $AERONET_{10am}$ (see Table 6 for variable definitions). In each model, $AERONET_{10am}$ was treated as a continuous variable, and all other factors were treated as categorical variables. The categorical variable in a given model may affect the model intercept and its interaction with $AERONET_{10am}$ may affect the model slope. The results were presented in the format of standard output of SAS procedure PROC GLM (Tables 7 and 8). For each model, the sample size and the model R^2 values were first reported. One level of the categorical variable and its interaction with $AERONET_{10am}$ were chosen as the reference state. The parameter estimates, the standard errors of the estimates and the significance levels were all calculated against the reference level.

Model No.1 in Table 7 was a simple linear regression between $MISR_{bestfit}$ and $AERONET_{10am}$ that served as the baseline model. The R^2 of 0.65 for the entire dataset indicated that $AERONET_{10am}$ explained the majority of the variation in $MISR_{bestfit}$. When using the entire dataset, a systematic positive error in $MISR_{bestfit}$ existed as evidenced from the positive intercept of 0.10 (± 0.01). Some possible explanations for the positive error might include: uncertainties related to the assumptions of aerosol models, inadequate cloud screening, imperfect aerosol climatology as well as the dependency on monthly averaged meteorological data rather than real time data. Quantitative

characterization of the positive error involved detailed analysis of MISR aerosol retrieval algorithm which is beyond the scope of this paper. The slope of 0.94 (±0.05) indicated that along the data range the two variables had a decent 1:1 relationship. This slope is comparable with the result using MODIS AOTs which yielded an error of ±0.05 on the intercept and ±0.2 on the slope [*Chu et al.*, 2002]. Regression analysis conducted using only four coastal sites (GSFC, MD Science Center, SERC and Cove, N = 61) found very similar result to that obtained using the full dataset. Both the intercept and slope in this case agree with the findings of *Chu et al.* [2002] at the US coastal sites.

Given the finding that $MISR_{bestfit}$ and $MISR_{regmean}$ are interchangeable, the model slope is also comparable with the results of *Diner et al*. [2001]. The higher error in the current analysis is probably due to the measurements in *Diner et al.* [2001] being taken at relatively dry and cloud free conditions, which contained less error from cloud contamination.

Model No.2 showed the seasonal effect on the relationship between $MISR_{bestfit}$ and $AERONET_{10am}$. In this model, *season* was a highly significant predictor of $MISR_{bestfit}$ although it only explained a small proportion of the variation (R^2 increased by 0.04 from baseline model). Differences in the intercept between fall and winter were not significant (0.06 ± 0.05) and likely reflected the systematic positive errors in $MISR_{bestfit}$. During the spring and summer, the error was even more pronounced (0.13 and 0.15 respectively). The interaction between *season* and $AERONET_{10am}$ was not significant so it was not included in the model. Results from this model suggest that the differences between the two AOT variables do not vary by season. In addition, since the mean $MISR_{bestfit}$ during the winter (0.11 ± 0.08) is almost comparable with the positive error, it is not surprising

to see the insignificant correlation between $MISR_{bestfit}$ and $AERONET_{10am}$ during the winter.

Model No.3 showed the impact of land use pattern on the relationship between $MISR_{bestfit}$ and $AERONET_{10am}$. *Urban* was a significant predictor ($p = 0.03$) of $MISR_{bestfit}$ and only explained a small proportion of the variation in MISR (R^2 increased by 0.01 from baseline model). In addition, the impact of the interaction between $AERONET_{10am}$ and *urban* on the model slope was significant ($p = 0.03$). In urban sites, the model had an intercept of 0.05 (± 0.04) and a slope of 1.12 (± 0.09). In suburban and rural sites, the intercept was 0.11 (± 0.01) and the slope is 0.88 (± 0.06).

Model No.4 showed the impact of aerosol size distribution on the relationship between the two AOT variables. *Dust* was a significant predictor of $MISR_{bestfit}$ ($p = 0.01$) although it only explained a small proportion of its variation (R^2 increased by 0.05 from baseline model). In addition, the interaction between $AERONET_{10am}$ and *dust* significantly affected the model slope ($p = 0.0002$) suggesting that the assumptions of aerosol size distributions in MISR retrieval have a strong impact on the accuracy of AOT values. This model had an intercept of 0.12 (± 0.06) and a slope of 0.43 (± 0.23) in coarse particle dominant scenarios. For fine particle dominant scenarios, model had an intercept of 0.04 (± 0.01) and a slope of 1.27 (± 0.17). For mixed type scenarios, model had an intercept of 0.14 (± 0.02) and a slope of 0.89 (± 0.05). In addition, *Urban* was found to be highly correlated with *dust* (Fisher's exact test, $p = 0.001$). This is likely because urban sites tend to be closer to anthropogenic emission therefore are more impacted by combustion sources but less by dust sources. As a result, both variables reflect the impact of aerosol size distribution on the agreement between $MISR_{bestfit}$ with

$AERONET_{10am}$. When both *dust* and *urban* as well as their interactions with $AERONET_{10am}$ were included in the model, *urban* and its interaction term became insignificant predictors of $MISR_{bestfit}$, suggesting that *dust* was probably a more accurate measure of aerosol size distribution than *urban*. When assessed together, the above results suggest that first, the error level in $MISR_{bestfit}$ varies by aerosol size distributions; second, the agreement between $MISR_{bestfit}$ and $AERONET_{10am}$ depends on AOT values; and finally coarse particles can strongly influence the quality of MISR AOT measurements.

As shown above, it is clear that a simple linear regression between $MISR_{bestfit}$ and $AERONET_{10am}$ could not fully explain their relationship therefore an expanded model including other factors such as *season* and *dust* was needed. When all present in the model, *dust*, *season*, and the interaction between *dust* and $AERONET_{10am}$ remained significant. Therefore, the following expanded model was finally chosen to describe the relationship between MISR and AERONET AOTs:

$$MISR_{bestfit} = \beta_0 + \beta_1 \times season + \beta_2 \times dust + \beta_3 \times AERONET_{10am} + \beta_4 \times dust \times AERONET_{10am}$$

In general, aerosol size distribution had a strong impact on the regression slopes while both seasonal and compositional effects were reflected on the intercepts (Table 8). The intercepts in the spring (0.16 ± 0.08) and summer (0.17 ± 0.09) were 0.07 – 0.08 greater than those in fall (0.09 ± 0.06) and winter (0.08 ± 0.09) (Table 9) likely reflecting the higher level of cloud contamination level during these two seasons. In addition, the intercepts, or the positive errors, were approximately 0.07 greater in the coarse particle dominant scenario and the mix particle scenario than in the fine mode dominant scenario. Since the intercepts of this expanded model can be interpreted as the positive error of

MISR AOTs uniformly distributed along the data range, the results suggested that MISR data had higher errors during the spring and summer and when coarse particles contribute a substantial fraction of AOT. The model slope of 0.46 (± 0.24) when coarse mode aerosol dominated the aerosol deviated substantially from the ideal slope of 1.0, likely caused by the low AOT values and high errors. Except in the coarse particle dominant scenario, which accounted for less than 10% of the data, the slope was within ± 16% of a 1:1 relationship. On average, higher intercepts were found during the summer and the lowest during the winter.

4. Conclusions

From the current analysis, it is clear that the MISR AOT parameters (best fit, regional mean and regional weighted mean AOTs) were interchangeable. AERONET AOTs measured between 10 and 11 a.m. were highly correlated with daylight averages, which suggest that MISR AOT measurements can represent daytime average aerosol abundance. In addition, MISR AOT retrievals had an overall positive error of approximately 0.10 as compared to AERONET measurements with no systematic bias across the observed data range. Regression analysis showed that the positive error was higher during the spring and summer or when coarse particles contribute substantially to AOT values. However, with MISR retrieval algorithm continuously being refined, these problems are expected to be addressed and MISR data quality will be improved. Except in the coarse particle dominant scenario, the regression slope of MISR against AERONET AOT varied between 0.84 and 1.16. Importantly, the overall good agreement between MISR and AERONET shows that MISR AOT data can be used as a quantitative

analysis tool for tropospheric aerosol research. Additionally, as aerosol optical properties can be related to $PM_{2.5}$ mass concentration, MISR data are especially promising for long-term $PM_{2.5}$ pollution monitoring at national or perhaps global scale.

Acknowledgements. This research is supported by Harvard University Center for the Environment (HUCE) Research Project Award and Harvard-EPA Center on Particle Health Effects (R827353-01-0). The authors would like to thank Dr. Vasu Kilaru for his help with data analysis in GIS. The authors would also like to thank the AERONET PIs for collecting the aerosol data over the U.S..

References

Bothwell, G.W., E.G. Hansen, R.E. Vargo, and K.C. Miller, The Multi-angle Imaging SpectroRadiometer science data system, its products, tools, and performance, *IEEE Trans. Geosci. Remote Sens.*, *40* (7), 1467-1476, 2002.

Bruegge, C., N. Chrien, R.R. Ando, D. Diner, W.A. Abdou, M.C. Helmlinger, S.H. Pilorz, and K.J. Thome, Early validation of the Multi-angle Imaging SpectroRadiometer (MISR) radiometric scale, *IEEE Trans. Geosci. Remote Sens.*, *40* (7), 1477-1492, 2002.

Chrien, N., C. Bruegge, and R.R. Ando, Multi-angle Imaging SpectroRadiometer (MISR) on-board calibrator (OBC) in-flight performance studies, *IEEE Trans. Geosci. Remote Sens.*, *40* (7), 1493-1499, 2002.

Chu, A., Y.J. Kaufman, C. Ichoku, L.A. Remer, D. Tanre, and B. Holben, Validation of MODIS aerosol optical depth retrieval over land, *Geophys.Res Lett.*, *29* (12), art no. 1617, 2002.

Diner, D., W. Abdou, C. Bruegge, J.E. Conel, K.A. Crean, B.J. Gaitley, M.C. Helmlinger, R. Kahn, J. Martonchik, and S.H. Pilorz, MISR aerosol optical depth retrievals over southern Africa during the SAFARI-2000 dry season campaign, *Geophys.Res Lett.*, *28* (16), 3127-3130, 2001.

Diner, D., J. Beckert, T.H. Reilly, C. Bruegge, J.E. Conel, R.A. Kahn, J. Martonchik, T.P. Ackerman, R. Davies, S.A.W. Gerstl, H. Gordon, J.-P. Muller, R.B. Myneni, P.J. Sellers, B. Pinty, and M.M. Verstraete, Multi-angle Imaging SpectroRadiometer

(MISR) Instrument Description and experiment overview, *IEEE Trans. Geosci. Remote Sens.*, *36* (4), 1072-1087, 1998.

Diner, D., J. Bruegge, J. Martonchik, T.P. Ackerman, R. Davies, S.A.W. Gerstl, H. Gordon, P.J. Sellers, J. Clark, J.A. Daniels, E.D. Danielson, V.G. Duval, K.P. Klaasen, G.W. Lilienthal, D.I. Nakamoto, R.J. Pagano, and T.H. Reilly, MISR: A Multiangle Imaging SpectroRadiometer for Geophysical and Climatological Research from Eos, *IEEE Trans. Geosci. Remote Sens.*, *27* (2), 200-214, 1989.

Eck, T.F., B. Holben, J. Reid, O. Dubovik, A. Smirnov, N.T. O'Neill, I. Slutsker, and S. Kinne, Wavelength dependence of the optical depth of biomass burning, urban, and desert aerosols, *J. Geophys. Res.*, *104* (D24), 31333-31349, 1999.

EPA, Latest findings on national air quality: 2001 status and trends, 2001.

Holben, B., T.F. Eck, I. Slutsker, D. Tanre, J.P. Buis, A. Setzer, E. Vermote, J.A. Reagon, Y.J. Kaufman, T. Nakajima, F. Lavenu, I. Jankowiak, and A. Smirnov, AERONET: A Federated Instrument Network and Data Archive for Aerosol Characterization, *Remote Sens. Environ.*, *66*, 1-16, 1998.

Hutchison, K.D., Applications of MODIS satellite data and products for monitoring air quality in the state of Texas, *Atmos. Environ.*, *37*, 2403-2412, 2003.

Jovanovic, V., M.A. Bull, M.M. Smyth, and J. Zong, MISR in-flight camera geometric model calibration and georectification performance, *IEEE Trans. Geosci. Remote Sens.*, *40* (7), 1512-1519, 2002.

JPL, Multi-angle Imaging Spectro-Radiometer Data Product Specifications, 2002.

Kahn, R., P. Banerjee, D. McDonald, and D. Diner, Sensitivity of multiangle imaging to aerosol optical depth and to pure-particle size distribution and composition over ocean, *J. Geophys. Res.*, *103* (D24), 32195-32213, 1998.

Kaufman, Y.J., D. Herring, K. Ranson, and G. Collatz, Earth Observing System AM 1 Mission to Earth, *IEEE Trans. Geosci. Remote Sens.*, *36* (4), 1045-1055, 1998.

Kaufman, Y.J., B.N. Holben, D. Tanre, I. Slutsker, A. Smirnov, and T.F. Eck, Will aerosol measurements from Terra and Aqua polar orbiting satellites represent the daily aerosol abundance and properties?, *Geophys.Res Lett.*, *27* (23), 3861-3864, 2000.

Martonchik, J.V., D.J. Diner, R.A. Kahn, T.P. Ackerman, M.M. Verstraete, B. Pinty, and H. Gordon, Techniques for the Retrieval of Aerosol properties Over Land and Ocean Using Multiangle Imaging, *IEEE Trans. Geosci. Remote Sens.*, *36* (4), 1212-1227, 1998.

O'Neill, N.T., A. Ignatov, B. Holben, and T.F. Eck, The lognormal distribution as a reference for reporting aerosol optical depth statistics; Empirical tests using multi-year, multi-site AERONET sunphotometer data, *Geophys.Res Lett.*, *27* (20), 3333-3336, 2000.

Smirnov, A., Cloud-Screening and Quality Control Algorithms for the AERONET Database, *Remote Sens. Environ.*, *73* (3), 337-349, 2000.

Thulasiraman, S., N.T. O'Neill, A. Royer, B. Holben, D. Westphal, and L.J.B. McArthur, Sunphotometric observations of the 2001 Asian dust storm over Canada and the US, *Geophys.Res Lett.*, *29* (8), art no. 1255, 2002.

Torres, O., P.K. Bhartia, J.R. Herman, A. Sinyuk, P. Ginoux, and B. Holben, A long-term record of aerosol optical depth from TOMS observations and comparison to AERONET measurements, *J. Atmos. Sci.*, *59* (3), 398-413, 2002a.

Torres, O., J.R. Herman, P.K. Bhartia, and A. Sinyuk, Aerosol properties from EP-TOMS near UV observations, *Advances in Space Research*, *29* (11), 1771-1780, 2002b.

Zhao, T.X., L. Stowe, A. Smirnov, D. Crosby, J. Sapper, and C. McClain, Development of a global validation package for satellite oceanic aerosol optical thickness retrieval based on AERONET observations and its application to NOAA/NESDIS operational aerosol retrievals, *J. Atmos. Sci.*, *59* (3), 294-312, 2002.

Figures Captions

Figure 1. Selected 16 AERONET sites in the contiguous US

Figure 2. Histograms of MISR and AERONET AOT parameters (sample size = 207 for all MISR variables)

Figure 3. Scatter plot of $MISR_{bestfit}$ vs. $AERONET_{10am}$ with three possible outliers in the circle

Figure 4. Full records of AERONET AOT interpolated to 550 nm and total precipitable water (TPW) for three periods at Walker Branch site

Figure 5. Summary statistics of $AERONET_{10am}$ (left box) and $MISR_{bestfit}$ (right box) at different AERONET sites. Big Meadows site (N = 2) and Harvard Forest site (N = 1) are not shown due to limited sample size

Figure 6. Scatter plots of $MISR_{regmean}$ vs. $MISR_{bestfit}$ (upper) and $MISR_{wgtdmean}$ vs. $MISR_{bestfit}$ (lower) as well as the results of simple linear regressions

Figure 7. Scatter plot of AERONET mean AOT vs. AOT at MISR time window and the result of simple linear regression

Tables

Table 1 Geographic information of selected AERONET sites in the US.

Site ID	Site name	State	Elevation (m)	Latitude (Degree)	Longitude (Degree)	Land use and land cover type*
1	Rogers Dry Lake	CA	680	34.926	117.885	Rural, grassland and shrub
2	La Jolla	CA	0	32.500	117.160	Urban, ocean, grassland and build-up land
3	Maricopa	AZ	0	33.071	111.972	Rural, shrub land
4	Servilleta	NW	1477	34.355	106.885	Rural, shrub land
5	CART	OK	315	36.610	97.410	Rural, dry land, crop land and pasture
6	Sioux Falls	SD	500	43.736	96.626	Rural, dry land, crop land and pasture
7	Stennis	MS	20	30.368	89.617	Rural, evergreen needle leaf forest, dry land, cropland and pasture
8	Bondville	IL	212	40.053	88.372	Rural, dry land, cropland and pasture
9	Walker Branch	TN	365	35.958	84.287	Suburban, broadleaf forest, build-up land
10	Big Meadows	VA	1082	38.522	78.436	Rural, mixed forest
11	GSFC	MD	50	39.030	76.880	Urban, build-up land
12	MD Science Center	MD	15	39.283	76.617	Urban, build-up land
13	SERC	MD	10	36.883	76.500	Suburban, broadleaf forest, ocean
14	Cove	VA	0	36.900	75.710	Ocean platform, 40 km from shore
15	Philadelphia	PA	20	40.036	75.005	Urban, build-up land
16	Harvard Forest	MA	322	42.532	72.188	Rural, broadleaf forest

Table 2. Yearly statistics for MISR and AERONET 550 nm AOTs

Variables	N[6]	Mean	Median	SD[7]	Max
$MISR_{bestfit}$ [1]	204	0.26	0.20	0.21	1.09
$MISR_{regmean}$ [2]	204	0.26	0.20	0.22	1.26
$MISR_{wgtdmean}$ [3]	204	0.26	0.21	0.21	1.13
$AERONET_{daily}$ [4]	204	0.16	0.10	0.16	0.85
$AERONET_{10am}$ [5]	204	0.17	0.10	0.18	1.08

[1] $MISR_{bestfit}$ refers to Best-fit MISR AOT at 550 nm.

[2] $MISR_{regmean}$ refers to Regional Mean MISR at AOT 550 nm.

[3] $MISR_{wgtdmean}$ refers to Weighted Regional Mean MISR at AOT 550 nm.

[4] $AERONET_{daily}$ refers to all day average AERONET AOT at 550nmg time.

[5] $AERONET_{10am}$ refers to AERONET AOT at 550 nm at MISR time window (10 - 11am local time)

[6] N refers to sample size.

[7] SD refers to arithmetic standard deviation.

Table 3. Seasonal statistics for MISR and AERONET AOT variables

	Spring					Summer				
Variables	N[1]	Mean	Median	SD[2]	Max	N	Mean	Median	SD	Max
$MISR_{bestfit}$	50	0.26	0.24	0.17	0.85	81	0.36	029	0.25	1.09
$MISR_{regmean}$	50	0.28	0.25	0.18	0.85	81	0.36	0.26	0.26	1.26
$MISR_{wgtdmean}$	50	0.27	0.25	0.18	0.85	81	0.36	0.28	0.25	1.13
$AERONET_{daily}$	50	0.15	0.13	0.11	0.40	81	0.24	0.15	0.20	0.85
$AERONET_{10am}$	50	0.16	0.12	0.12	0.63	81	0.25	0.15	0.24	1.08
	Fall					Winter				
$MISR_{bestfit}$	41	0.17	0.13	0.12	0.45	32	0.11	0.08	0.08	0.36
$MISR_{regmean}$	41	0.17	0.13	0.12	0.47	32	0.11	0.10	0.07	0.38
$MISR_{wgtdmean}$	41	0.17	0.13	0.11	0.46	32	0.11	0.09	0.07	0.42
$AERONET_{daily}$	41	0.12	0.08	0.11	0.55	32	0.06	0.05	0.04	0.16
$AERONET_{10am}$	41	0.13	0.08	0.14	0.76	32	0.06	0.06	0.03	0.14

[1] N refers to sample size.

[2] SD refers to arithmetic standard deviation.

Table 4. Descriptive statistics for MISR and AERONET AOT variables at different aerosol size distributions

	Coarse mode dominant				
Variables	N[1]	Mean	Median	SD[2]	Max
$MISR_{bestfit}$	19	0.18	0.16	0.11	0.45
$MISR_{regmean}$	19	0.20	0.16	0.12	0.47
$MISR_{wgtdmean}$	19	0.19	0.16	0.11	0.40
$AERONET_{10am}$	19	0.12	0.09	0.16	0.76
$AERONET_{daily}$	19	0.11	0.10	0.12	0.55
	Mix of coarse and fine mode				
$MISR_{bestfit}$	116	0.29	0.21	0.24	1.09
$MISR_{regmean}$	116	0.30	0.23	0.23	1.08
$MISR_{wgtdmean}$	116	0.30	0.24	0.23	1.05
$AERONET_{10am}$	116	0.20	0.11	0.21	1.08
$AERONET_{daily}$	116	0.19	0.11	0.19	0.85
	Fine mode dominant				
$MISR_{bestfit}$	69	0.22	0.17	0.19	1.09
$MISR_{regmean}$	69	0.22	0.17	0.20	1.26
$MISR_{wgtdmean}$	69	0.22	0.17	0.19	1.13
$AERONET_{10am}$	69	0.15	0.11	0.13	0.79
$AERONET_{daily}$	69	0.14	0.11	0.19	0.71

[1] N refers to sample size.

[2] SD refers to arithmetic standard deviation.

Table 5. Spearman's correlations coefficients (r) between $MISR_{bestfit}$ and AERONET $AERONET_{10am}$ at different AERONET sites and the significance levels of r.

Site Name[1]	State	N	r	Prob > |r| under H0: Rho=0
Rogers Dry Lake	CA	26	0.37	0.06
Bondville	IL	19	0.51	0.02
Servilleta	NM	19	0.59	0.008
Maricopa	AZ	17	0.63	0.006
La Jolla	CA	9	0.70	0.04
Cove	VA	15	0.74	0.002
Walker Branch	TN	17	0.79	0.0002
CART	OK	9	0.82	0.007
Philadelphia	PA	12	0.89	0.0001
MD Science Center	MD	18	0.91	< 0.0001
SERC	MD	10	0.93	0.0001
GSFC	MD	18	0.94	< 0.0001

[1] Calculation was only conducted at sites with no less than 9 observations.

Table 6. Correlations coefficients (r) between MISR and AERONET by different classifications.

Classification	Value	N	r	Prob > |r| under H0: Rho=0
West[1]	1 (west coast)	45	0.54	< 0.0001
	2 (midwest)	57	0.73	< 0.0001
	3 (east coast)	76	0.89	< 0.0001
Season[2]	1 (winter)	32	0.22	0.21
	2 (spring)	50	0.56	< 0.0001
	3 (summer)	81	0.79	< 0.0001
	4 (fall)	41	0.59	< 0.0001
$Flag_{MISR}$ [3]	7	122	0.58	< 0.0001
	8	82	0.83	< 0.0001
Altitude[4]	1 (high)	53	0.50	< 0.0001
	2 (low)	151	0.80	< 0.0001
Urban[5]	1 (urban)	57	0.90	< 0.0001
	2 (suburban and rural)	147	0.69	< 0.0001
Dust[6]	1 (coarse)	19	0.39	0.10
	2 (fine)	69	0.78	< 0.0001
	3 (mixture)	116	0.75	< 0.0001

[1]*West* is the classification for the geographic locations of AERONET sites. West = 1 for western sites (Rogers Dry Lake, La Jolla, Maricopa and Sevilleta); West = 2 for mid west sites (CART, Sious Falls, Bondville, Walker Branch, and Big Meadows); West = 3 for eastern sites (GSFC, MD Science Center, SERC, Cove, Philadelphia and Harvard forest).

[2]*Season* is the classification for seasonal effect. Season = 1 for December, January and February; season = 2 for March, April and May; season = 3 for June, July and August; season = 4 for September, October and November.

[3]$Flag_{MISR}$ is the classification for MISR data quality. FlagMISR = 7 if MISR retrieval over a pixel is successful; MISR flag = 8 if MISR retrieval over a pixel is not successful and the average of 3×3 pixels is given.

[4]*Altitude* is the classification for different elevations of AERONET sites. Altitude = 1 if the elevation of an AERONET site is higher than 400m, otherwise altitude = 2.

[5]*Urban* is the classification for the land use types of AERONET sites. Urban = 1 for urban sites, and urban = 2 otherwise.

[6]*Dust* is the classification for different aerosol size distribution. Dust = 1 for coarse particle dominant scenarios (Angstrom exponent < 0.75), dust = 2 for fine particle dominant scenarios (Angstrom exponent > 1.70), dust = 3 for mixtures of coarse and fine particles (0.75 < Angstrom exponent < 1.70).

Table 7. Outputs of SAS PROC GLM for various models: Fit statistics and model estimates of the models of predicting $MISR_{bestfit}$ using (1) AERONET alone for the entire dataset (N = 204) and four coastal sites in eastern US (N = 61), (2) AERONET and seasonal effects, (3) AERONET, land use type and their interaction, and (4) AERONET, aerosol type and their interaction.

Model	N	R^2	Parameter*	Estimate	StdErr[1]	p value [2]
1	204	0.65	Intercept	0.10	0.01	< 0.0001
			$AERONET_{10am}$	0.94	0.05	< 0.0001
	61	0.78	Intercept	0.08	0.02	0.0004
			$AERONET_{10am}$	0.95	0.07	< 0.0001
2	204	0.69	Intercept	0.06	0.02	0.006
			$AERONET_{10am}$	0.86	0.05	< 0.0001
			season = 1 (Winter)	-0.001	0.03	0.96
			season = 2 (Spring)	0.07	0.02	0.006
			season = 3 (Summer)	0.10	0.02	< 0.0001
			season = 4 (Fall)**	0.00	N/A	N/A
3	204	0.66	Intercept	0.11	0.01	< 0.0001
			$AERONET_{10am}$	0.88	0.06	< 0.0001
			urban = 1 (urban)	-0.06	0.03	0.03
			urban ** =2 (suburban and rural)	0.00	N/A	N/A
			$AERONET_{10am} \times urban^3$ (urban = 1)	0.24	0.11	0.03
			$AERONET_{10am} \times urban$ ** (urban = 2)	0.00	N/A	N/A
4	204	0.69	Intercept	0.12	0.02	< 0.0001
			$AERONET_{10am}$	0.89	0.05	< 0.0001
			dust = 1 (coarse)	0.008	0.04	0.83
			dust = 2 (fine)	-0.08	0.03	0.004
			dust = 3 (mixture)	0.00	N/A	N/A
			$AERONET_{10am} \times dust^4$ (dust = 1)	-0.47	0.19	0.01
			$AERONET_{10am} \times dust$ (dust = 2)	0.38	0.12	0.003
			$AERONET_{10am} \times dust$** (dust = 3)	0.00	N/A	N/A

* Definitions of variables are given in Table 6.

** Reference states.

[1] StdErr stands for the stand error the parameter estimate.

[2] p value standards for the significance level of the parameter estimate against the reference state.

[3] $AERONET_{10am}$ × urban stands for the interaction term between $AERONET_{10am}$ and categorical variable *urban*.

[4] $AERONET_{10am}$ × dust stands for the interaction term between $AERONET_{10am}$ and categorical variable *dust*.

Table 8. Fit statistics and model estimates of the models of predicting $MISR_{bestfit}$ using $AERONET_{10am}$, *dust, season* and their interaction with $AERONET_{10am}$ as predictors.

N	R^2	Parameter**	Estimate	StdErr	t Value	Prob t
		Intercept	0.08	0.02	3.49	0.0006
		$AERONET_{10am}$	0.83	0.05	15.53	<0.0001
		dust = 1 (coarse)	0.01	0.04	0.37	0.71
		dust = 2 (fine)	-0.06	0.03	-2.43	0.02
		dust = 3 (mixed)*	0.00	N/A	N/A	N/A
204	0.71	*season* = 1 (winter)	-0.008	0.03	-0.30	0.76
		season =2 (spring)	0.06	0.02	2.42	0.02
		season = 3 (summer)	0.08	0.02	3.17	0.002
		season =4 (fall)*	0.00	N/A	N/A	N/A
		$AERONET_{10am}$ × dust (dust = 1)	-0.38	0.18	-2.07	0.04
		$AERONET_{10am}$ × dust (dust = 2)	0.33	0.12	2.70	0.008
		$AERONET_{10am}$ × dust (dust = 3)*	0.00	N/A	N/A	N/A

* Reference state.

** Definitions of variables are given in Table 6.

Table 9. Estimates of the intercepts and slopes in each combination of aerosol size distribution and season from the final GLM.

Size distribution	Season			
	Winter	Spring	Summer	Fall
Coarse mode dominant	4[a] 0.08[b] (0.09[c]) 0.46[d] (0.24[e])	7 0.16 (0.09) 0.46(0.24)	2 0.17 (0.08) 0.46(0.24)	6 0.09 (0.06) 0.46(0.24)
Fine mode dominant	11 0.01 (0.08) 1.16 (0.18)	14 0.08 (0.07) 1.16 (0.18)	25 0.09 (0.07) 1.16 (0.18)	19 0.02 (0.05) 1.16 (0.18)
Mix of coarse and fine	17 0.07 (0.05) 0.84 (0.05)	29 0.14 (0.05) 0.84 (0.05)	54 0.16 (0.05) 0.84 (0.05)	16 0.08 (0.03) 0.84 (0.05)

[a] Number of records in this cell.

[b] Estimated intercept.

[c] Standard error of the estimate of the intercept.

[d] Estimated slope.

[e] Standard error of the estimate of the slope.

Figures

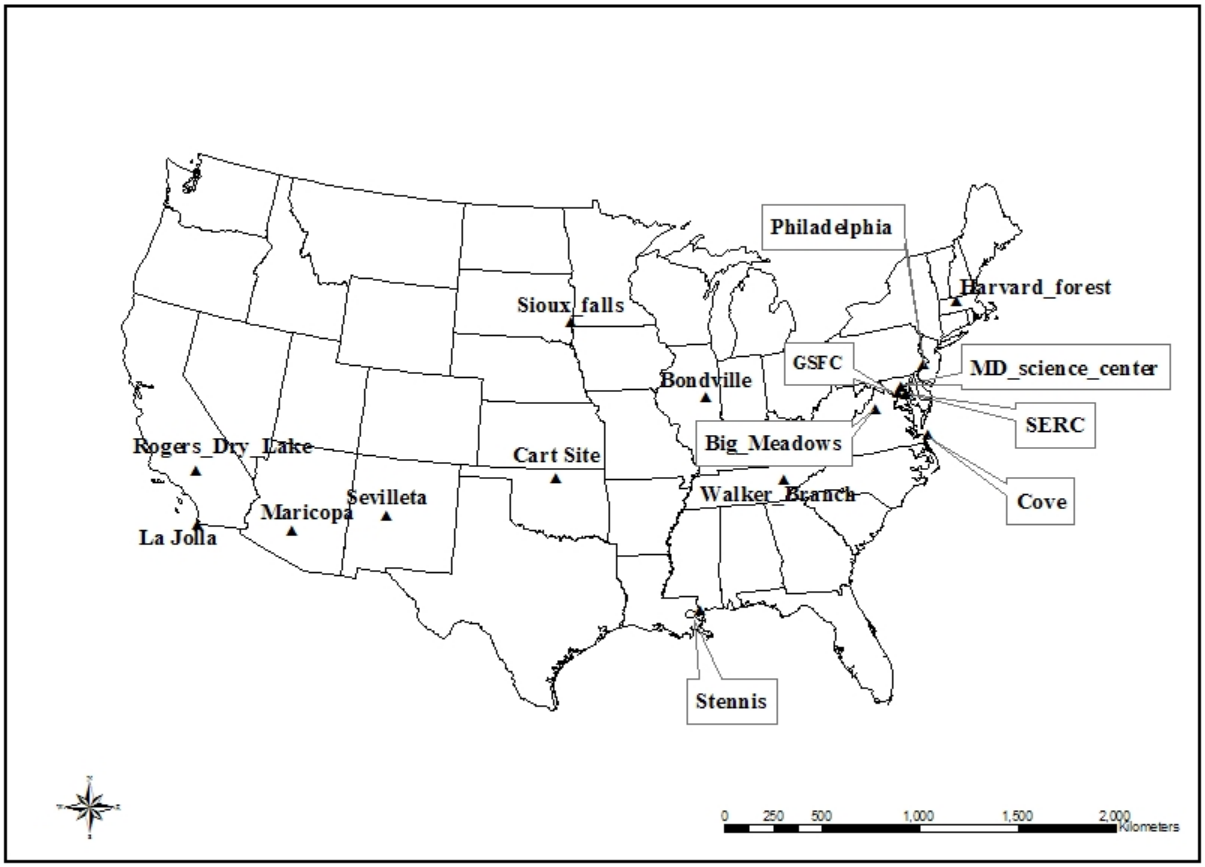

Figure 1 Selected 16 AERONET sites in the contiguous US

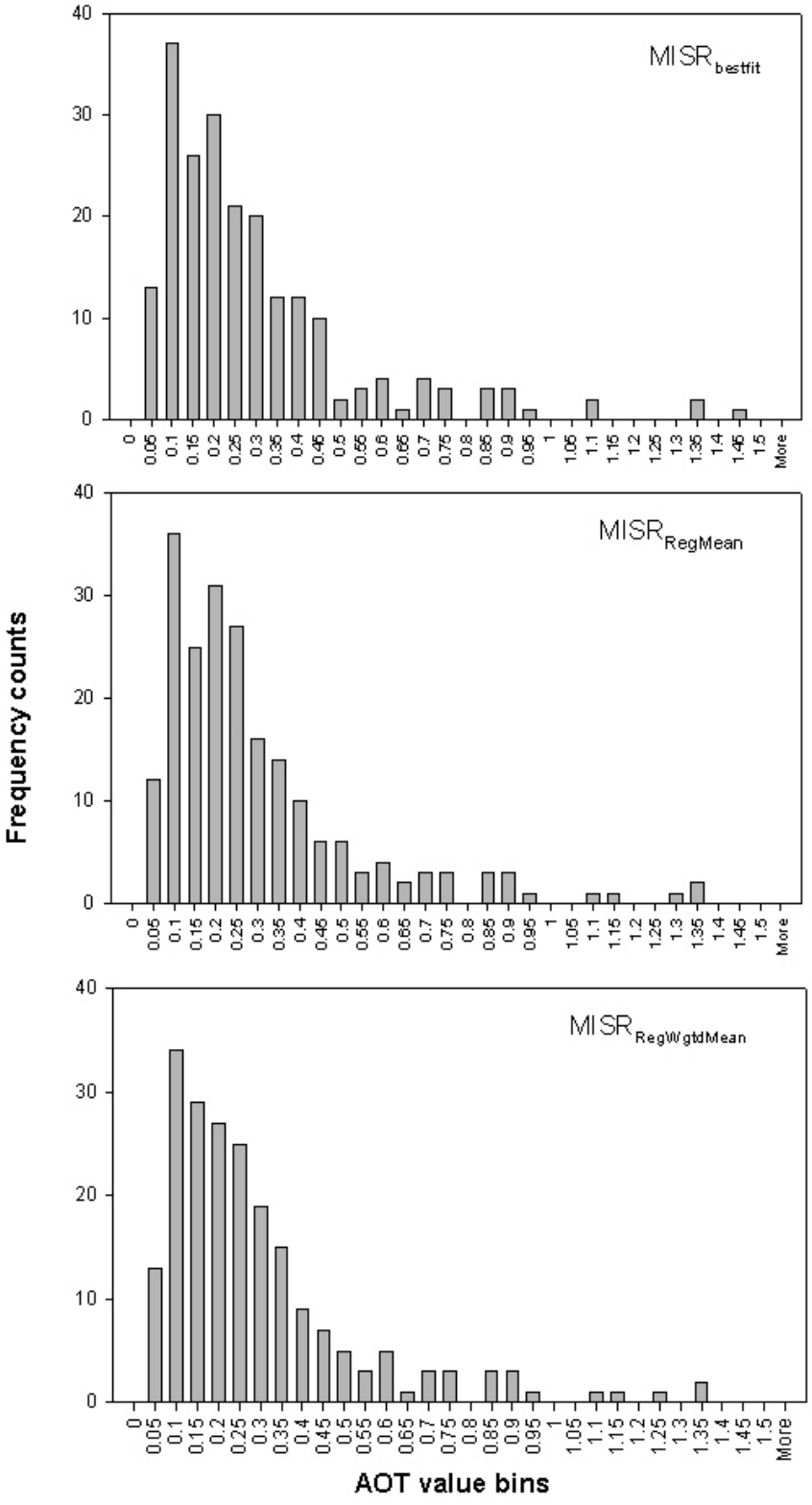

Figure 2. Histograms of MISR and AERONET AOT parameters (sample size = 207 for all MISR variables)

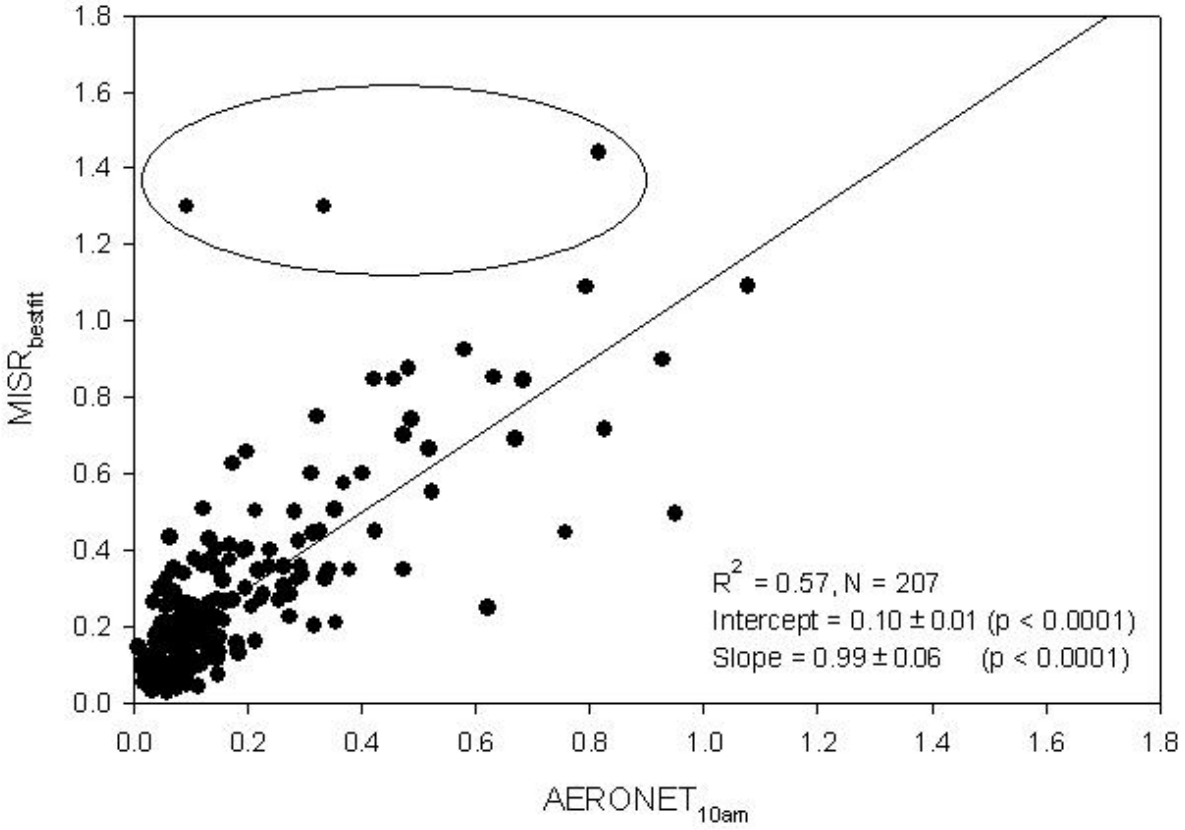

Figure 3. Scatter plot of $MISR_{bestfit}$ vs. $AERONET_{10am}$ with three possible outliers in the circle.

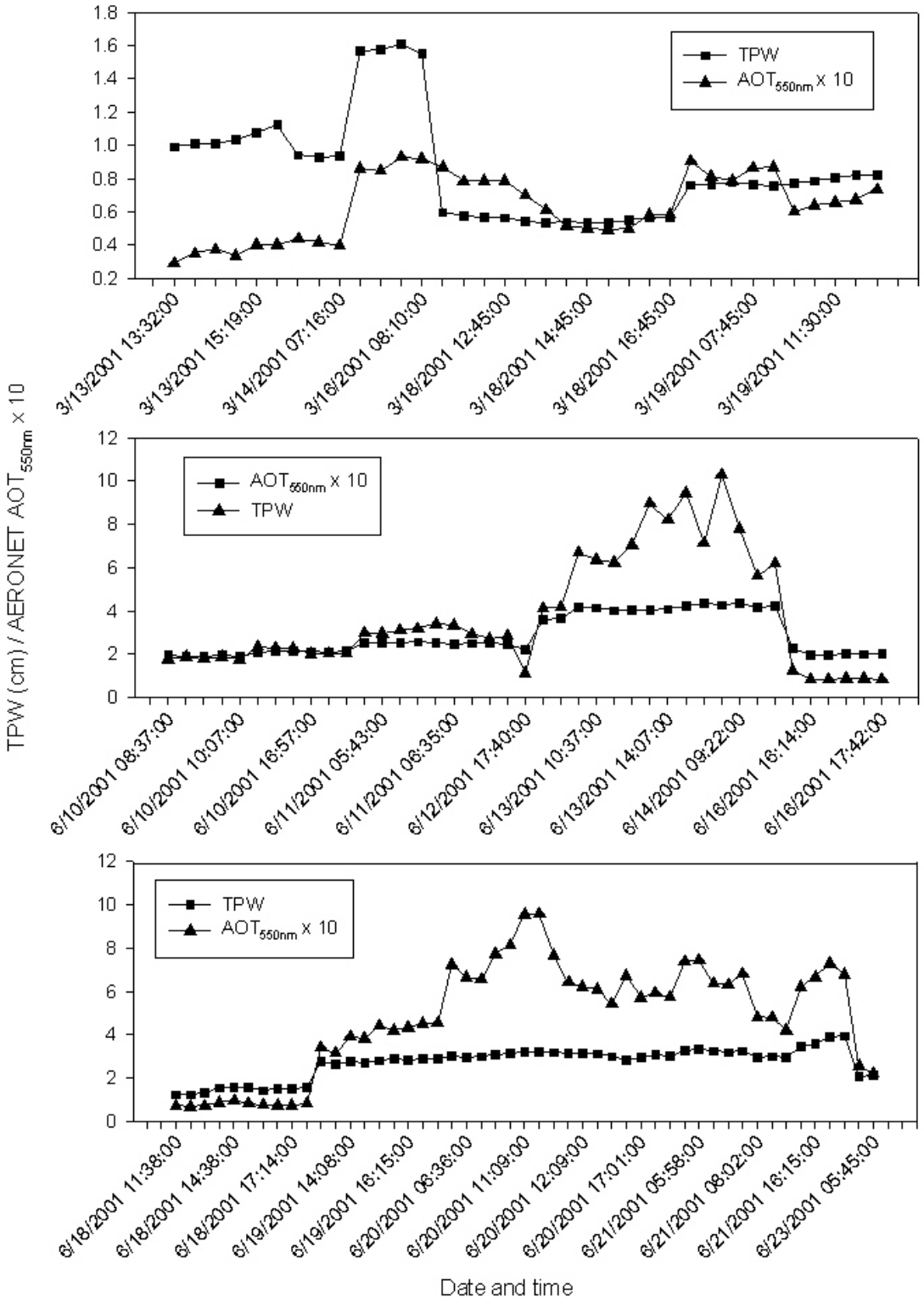

Figure 4. Full records of AERONET AOT interpolated to 550 nm and total precipitable water (TPW) for three periods at Walker Branch site.

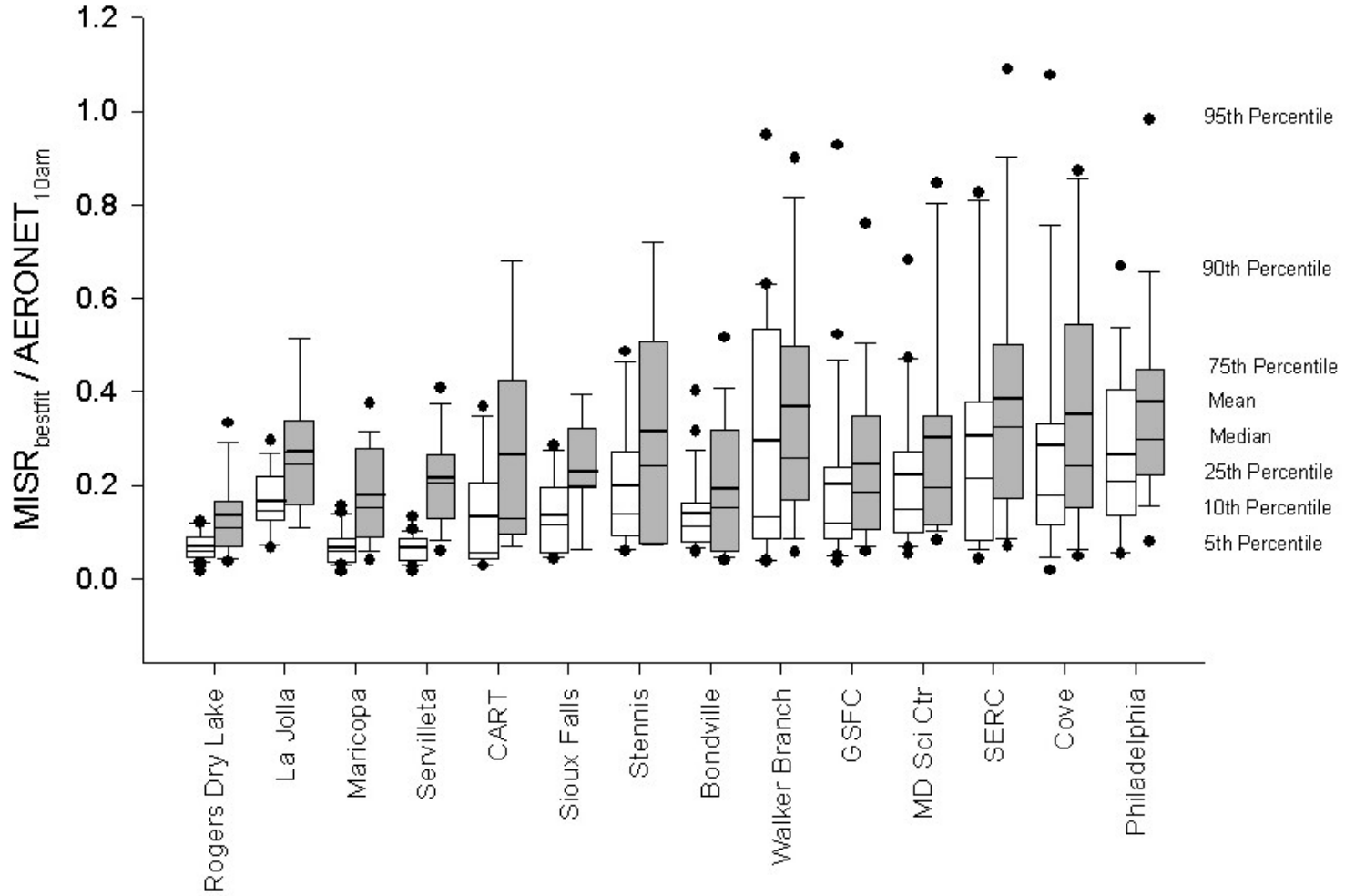

Figure 5. Summary statistics of $AERONET_{10am}$ (left box) and $MISR_{bestfit}$ (right box) at different AERONET sites. Big Meadows site (N = 2) and Harvard Forest site (N = 1) are not shown due to limited sample size.

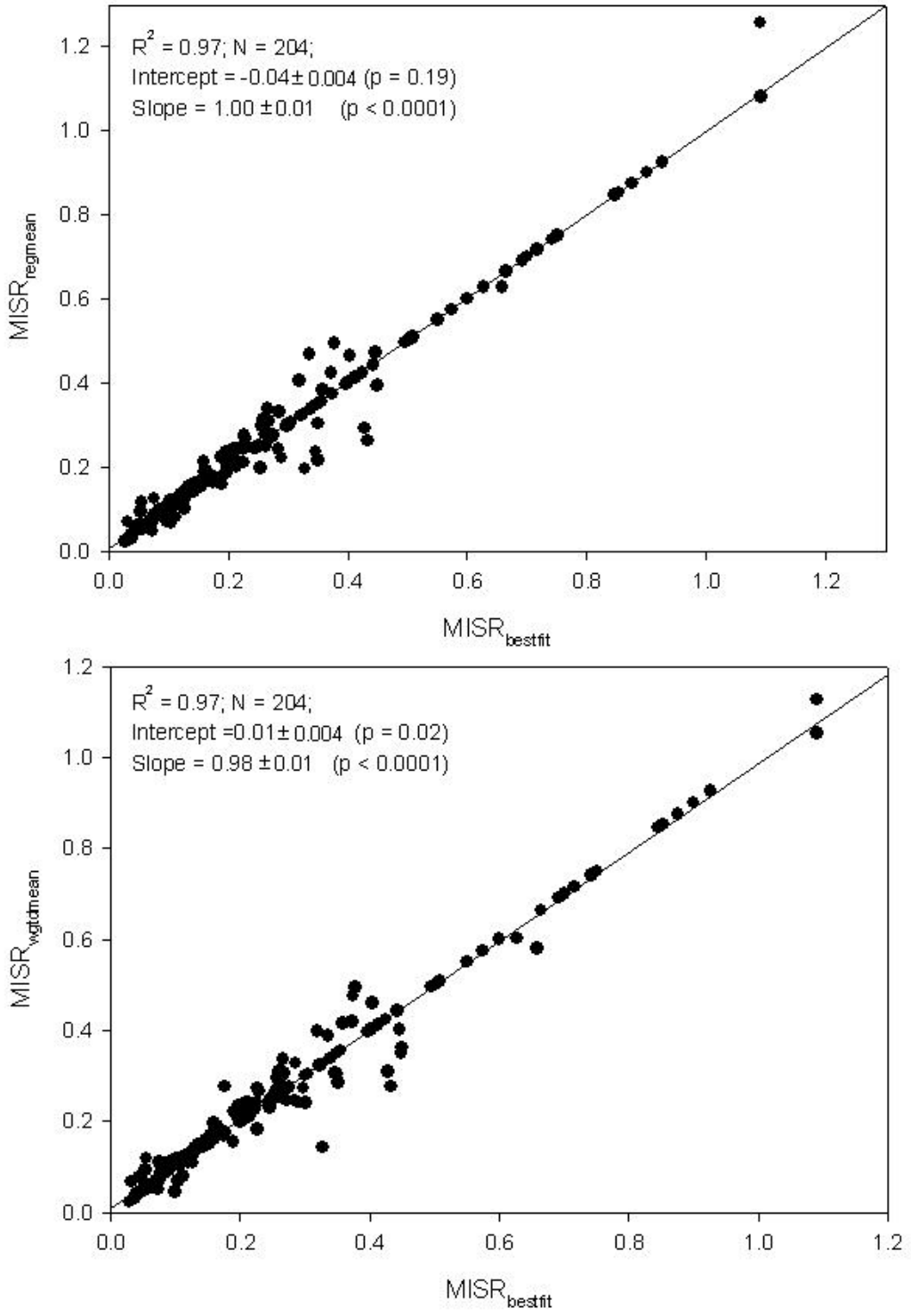

Figure 6. Scatter plots of $MISR_{regmean}$ vs. $MISR_{bestfit}$ (upper) and $MISR_{wgtdmean}$ vs. $MISR_{bestfit}$ (lower) as well as the results of simple linear regressions.

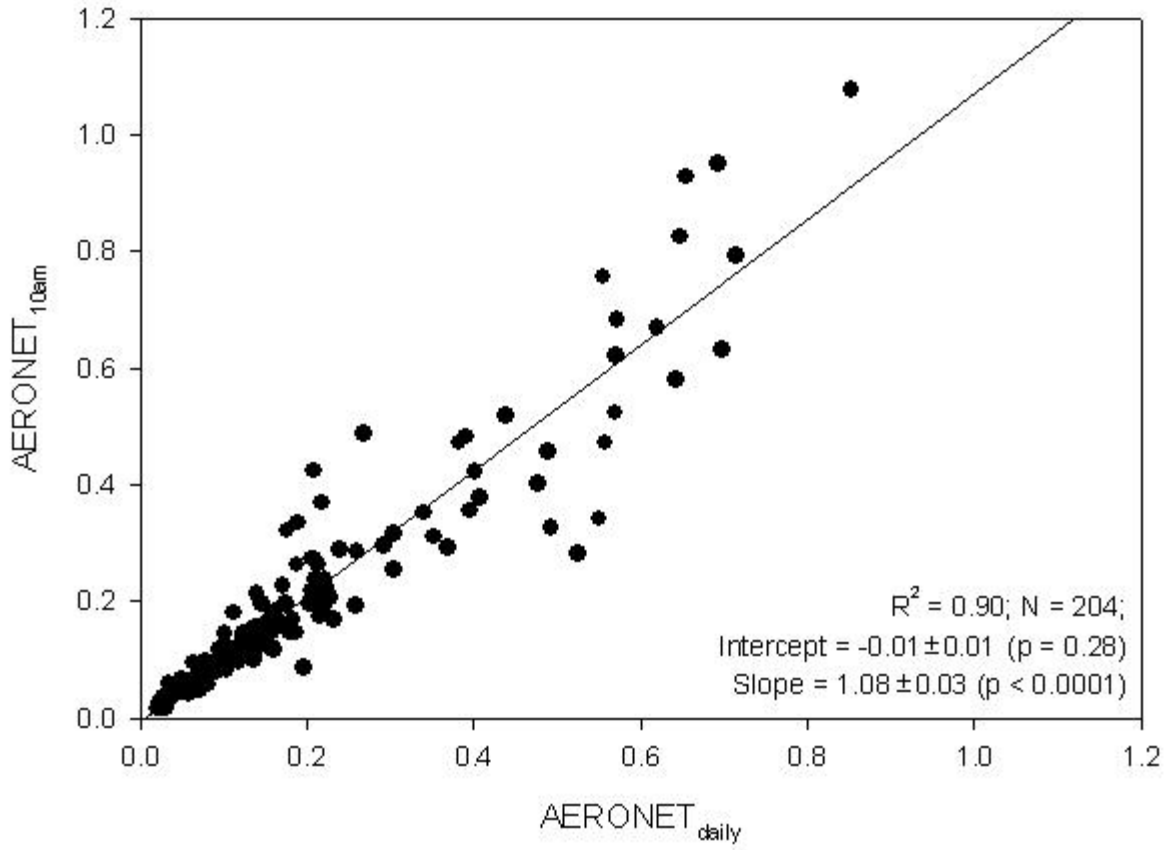

Figure 7. Scatter plot of AERONET mean AOT vs. AOT at MISR time window and the result of simple linear regression.